World Conference on Timber Engineering Oslo 2023

EFFICIENT FINITE ELEMENT MODELS FOR ADHESIVE-FREE MULTI-LAYERED TIMBER STRUCTURES

J. Paroissien[1,2], T.A. Bui[3], M. Oudjene[1], P. Lardeur[2]

ABSTRACT: This paper presents finite element models to assess the vibration performance of multi-layered timber structures assembled through compressed wood dowels. Starting from a solid model which is considered as a reference, a new methodology using a solid-beam approach for the dowels and a solid-shell approach for the layers is described. Kinematic assumptions are applied throughout the cross-section of the dowels and the thickness of layers, leading to a significant reduction of the number of variables. The models are assessed for the calculation of frequencies and mode shapes of multi-layered timber beams and timber panels. The efficiency of this approach, in terms of quality of results and model size, is highlighted.

KEYWORDS: timber construction, wood dowels, finite element, solid-shell, solid-beam.

1 INTRODUCTION

The construction sector faces an increasing need for more sustainable materials. This is brought together by institutions that impose increasingly stringent standards and consumers who transform the market through their more ecological demands.

Adhesive-free multi-layered timber structures aim to replace glue-laminated timber structures as an eco-friendly alternative by improving their durability and recyclability. Indeed, at high temperatures, glue emits toxic gases, especially formaldehyde which is carcinogenic to humans [1].

A concern for timber construction is the vibration serviceability of timber floors, glued or not. Human activity and children jumping in a residential or commercial building induce annoying vibrations in timber floors since they are lightweight structural elements.

Bui et al. [2,3] performed an experimental and numerical investigation on the vibration performance of Adhesive-Free Laminated Beams (AFLB) (Figure 1) and Adhesive-Free Cross-Laminated Timber (AFCLT) panels (Figure 2) assembled through compressed wood dowels.

Namely, this study highlighted a high variability level of frequencies. A finite element model made of solid elements was proposed for the layers and the dowels. Bui et al. [4] developed the Modal Stability Procedure (MSP) for the evaluation of the variability of frequencies, using this solid finite element model. This model is satisfactory in terms of quality of results but is time-consuming, particularly in the context of variability assessment or optimization where a large number of analyses may be necessary.

Figure 1: *Manufactured Adhesive-Free Laminated Beam (AFLB) [5]*

Figure 2: *Manufactured Adhesive-Free Cross-Laminated Timber (AFCLT) panels [5]*

[1] Université Laval, Département de Génie Civil et de Génie des Eaux, Faculté des Sciences et de Génie, Québec, Canada, marc.oudjene@gci.ulaval.ca

[2] Université de Technologie de Compiègne, Laboratoire Roberval, Compiègne, France, pascal.lardeur@utc.fr

[3] Kumoh National Institute of Technology, Gyeongbuk, South Korea, tuan-anh.bui@kumoh.ac.kr

https://doi.org/10.52202/069179-0343

Models using classical beam elements for the dowels and classical shell elements for the layers were tested by Bui [5]. These models lead to several difficulties, namely due to the complex deformation of dowels and the specific geometry representation, and are finally unsatisfactory.
Solid-shell and solid-beam approaches were developed by Wei et al. [6,7]. These approaches have the advantages to use solid elements and to reduce the number of degrees of freedom in a model by applying beam or shell theories.
These approaches are applicable to AFLB and AFCLT panels to reduce the model while keeping the solid geometry of the structure. However, adapting the solid-shell and solid-beam approaches to industrial structures is a novelty.
In this paper, we first recall the main experimental results obtained for AFLB and AFCLT panels. Then we present the reference finite element model of multi-layered timber beams and timber panels for modal analysis in free-free conditions. To reduce computational time using these reference models, reduced models using solid-beam and solid-shell approaches are also presented. Finally, a method to calculate variability is described.

2 SUMMARY OF EXPERIMENTAL DATA

In Bui et al. study [2], two wood species were considered for the layers: spruce and oak. The experimental campaign and the results were obtained in free-free conditions to minimize boundary conditions effects, with the hammer impact technique. The experimental set-up for the assessment of vibration behavior of AFLB and AFCLT panels is shown in Figure 3.

(a)

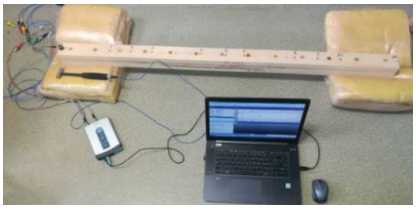

(b)

Figure 3: *Experimental set-up for (a) AFLB, (b) AFCLT panels [5]*

For the beams, 11 measurement points are chosen along the longitudinal axis, and for the panels 15 measurement points are distributed over the whole surface.
In this paper, we consider AFLB and AFCLT panels composed of oak for the layers and compressed spruce for the dowels. The moisture content during the experiments was 9 %.
The first three bending modes for both types of structures are presented.
The AFLB pictured in Figures 1 and 3a is composed of three oak layers and 27 compressed spruce dowels. The beam has a length of 1450 mm for a width of 70 mm and a height of 67.5 mm.
The results for the experimental mean natural frequencies, damping ratios and their respective coefficients of variation are summarized in Table 1 for five AFLBs and Table 2 for five AFCLT panels.

Table 1: *Experimental natural frequencies and damping ratios [2] for five AFLBs*

		Mean value	CoV (%)
f1	frequency (Hz)	118.2	6.0
	damping (%)	4.3	9.0
f2	frequency (Hz)	281.0	5.3
	damping (%)	2.1	4.6
f3	frequency (Hz)	471.1	4.2
	damping (%)	1.9	13.7

The vibrational serviceability performance of AFLB was demonstrated by comparison to their glued counterparts by Bui et al. [5]. It was proved that while the difference between frequencies increase slightly with higher modes, the damping ratio is much higher for AFLB.
The AFCLT panels pictured in Figures 2 and 3b are composed of three oak layers, 28 boards and 196 compressed spruce dowels in total. Each external layer contains 7 boards, while the interior one contains 14 boards in the perpendicular direction. These panels have a length of 2100 mm for a width of 1050 mm and a height of 75 mm.

Table 2: *Experimental natural frequencies and damping ratios [2] for five AFCLT panels*

		Mean	CoV (%)
f_2	frequency (Hz)	54.5	2.5
	damping (%)	0.72	10.8
f_3	frequency (Hz)	56.3	8.5
	damping (%)	0.87	13.7
f_7	frequency (Hz)	110.3	3.0
	damping (%)	0.97	6.9

The vibrational characteristics for the assembled beams and panels show high variability levels as stated before. This highlights the need for a complete variability assessment of the structures.

https://doi.org/10.52202/069179-0343

3 REFERENCE FINITE ELEMENT MODEL

3.1 FINITE ELEMENT MODEL

The models for both AFLB and AFCLT panel using the Verification and Validation methods [8] are presented.
Finite element models are created using the software Abaqus/Standard©, and the twenty-node hexahedral solid element with reduced integration (C3D20R of Abaqus [9]) is exploited. After testing several solid elements, this choice has been made as it is the most efficient for convergence of frequencies and leads to a minimization of model size for these timber structures.
As finite element models must be as close as possible to the physical reality, assumptions based on experimental observations [2] related to the connection between the different parts, are made. On the one hand, in the following models, there are no interactions between the boards or the layers with each other. On the other hand, as the dowels are densified and tend to expand to keep their shape memory, contact without sliding is considered. Because meshes of layers and dowels are not coincident at their interfaces, the interaction between dowels and layers must be modelled. To stick the surfaces of the dowels and holes of the boards, the *Tie* option in Abaqus is chosen.
Finally, the mechanical properties of the oak boards, are a mix of experimental results from [2] for the density and the longitudinal modulus. For all the other elastic properties, empirical relations from Jodin's book [10] are used. For the compressed wood that constitutes the dowels, the properties were identified using a quasi-inverse problem by Bouhala et al. [11].

3.2 VERIFICATION STEP

The Verification process is completed when the convergence of frequencies to the accurate solution is achieved. For the Verification stage, a highly accurate solution is obtained with a very fine model as no analytical solution exists.
For the AFLB the results of the convergence study given in Figure 4 lead to an optimal mesh with about 13 000 elements and 220 000 degrees of freedom.
This model is described in Figure 5. It is important to note that in the dowels the mesh is refined near the interfaces between layers as shear stress gradients are high in these areas.
The same method is applied to the AFCLT panel. In particular, the same refinement technique is applied to the dowels. The convergence study illustrated in Figure 6 leads to an optimal mesh with about 86 000 elements and 1 500 000 degrees of freedom. This mesh is shown in Figure 7.

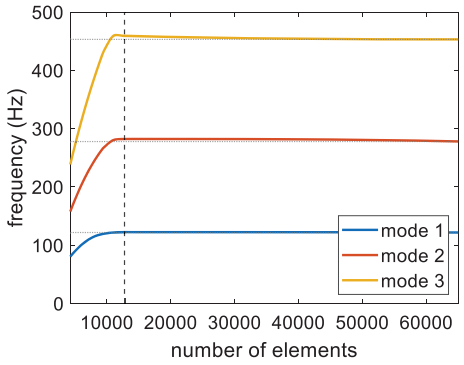

Figure 4: *Convergence study for AFLB*

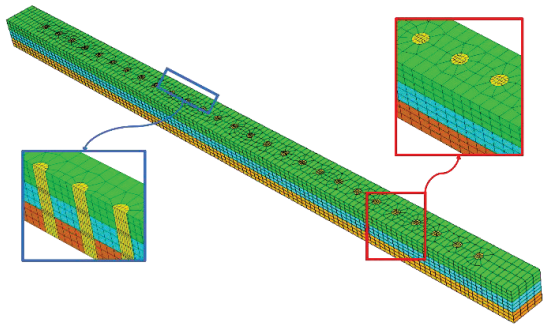

Figure 5: *AFLB finite element model*

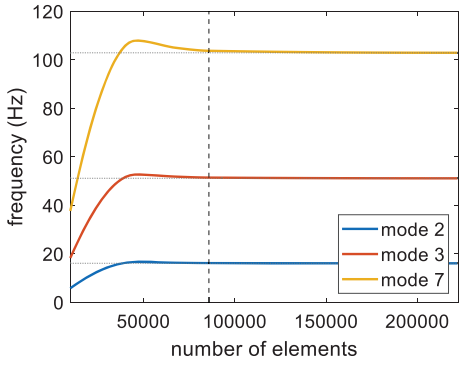

Figure 6: *Convergence study for AFCLT panel*

Table 3: *Elastic mechanical properties for dowels and layers*

	E_1 (MPa)	E_2 (MPa)	E_3 (MPa)	G_{12} (MPa)	G_{13} (MPa)	G_{23} (MPa)	ν_{12}	ν_{13}	ν_{23}
Oak [2,10]	11 380	1 045	1 871	977	1 275	361	0.4	0.32	0.43
Compressed spruce [11]	26 000	1 033	1 082	800	800	100	0.41	0.41	0.37

https://doi.org/10.52202/069179-0343

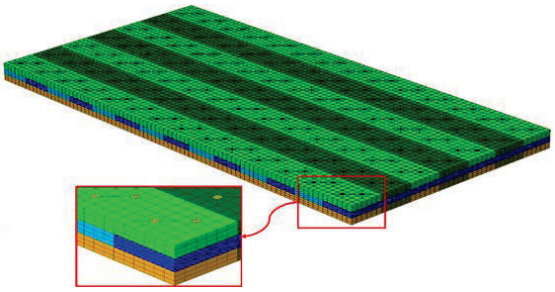

Figure 7: *AFCLT panel finite element model*

3.3 VALIDATION STEP

The Validation stage deals with the comparison between the numerical results obtained with the verified finite element model (from the previous Verification step) and the experimental results. As stated in section 2, we consider three frequencies that correspond to the first three bending modes illustrated in Figure 8 for the beam and Figure 9 for the panel.

Here, the Validation concerns only the mean behaviour of the structures, so numerical frequencies are compared to the mean experimental frequencies. Results are shown in Table 4 for AFLB and Table 5 for AFCLT panel.

Table 4: *Frequencies comparison between mean experimental data [2] and finite element model for AFLB*

	Mean experimental frequencies	Numerical frequencies	Diff.
f_1	118.2 Hz	119.1 Hz	0.7 %
f_2	281.0 Hz	278.2 Hz	-1.0 %
f_3	471.1 Hz	459.6 Hz	-2.4 %

Table 5: *Frequencies comparison between mean experimental data [2] and finite element model for AFCLT panel*

	Mean experimental frequencies	Numerical frequencies	Diff.
f_2	54.5 Hz	54.3 Hz	-0.3 %
f_3	56.3 Hz	55.9 Hz	-0.7 %
f_7	110.3 Hz	108.6 Hz	-1.6 %

Numerical and mean experimental results are in good agreement both for AFLB and AFCLT panel.

The small errors between numerical and experimental frequencies demonstrate that the adopted interaction assumptions are relevant despite that they may be questionable with regard to the complex physics involved in the connections.

This finite element modelling may lead to large-size models. In order to reduce the model size, a new methodology based on specific solid-beam and solid-shell approaches was developed.

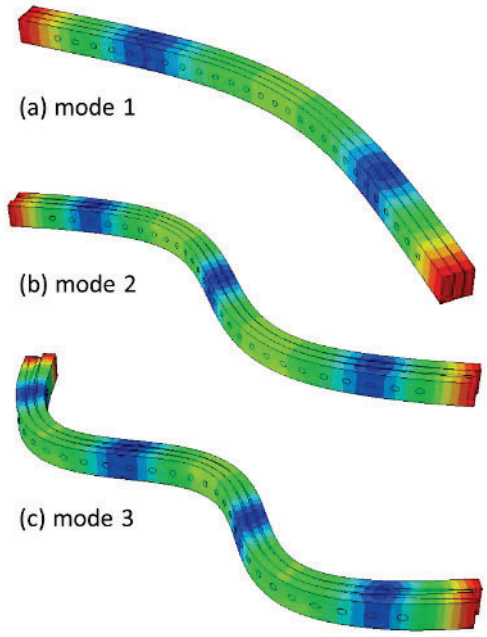

Figure 8: *Mode shapes for AFLB finite element model*

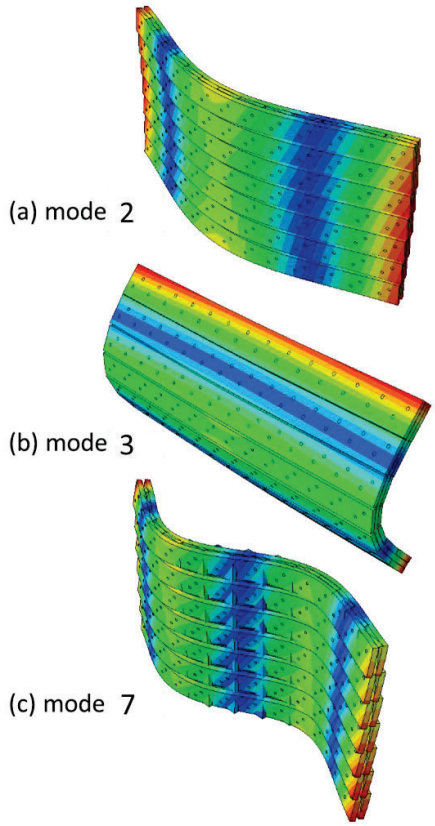

Figure 9: *Mode shapes for AFCLT panel finite element model*

https://doi.org/10.52202/069179-0343

4 SOLID-BEAM AND SOLID-SHELL BASED MODELS

4.1 PRINCIPLE OF SOLID-SHELL AND SOLID-BEAM APPROACHES

The solid-beam and solid-shell approaches used to build a reduced model exploit a methodology that was initially developed by Wei et al. [6,7].

The structure is first modelled with solid finite elements, for layers as well as dowels. Shell theory is considered for the layers and beam theory for the dowels. Then for layers, through-the-thickness shell equations are applied directly to the solid model. In the same way, through-the-section beam equations are applied for dowels. The concept of master and slave nodes is used, only master nodes are kept in the final model and slave nodes are eliminated. This process modifies the system of algebraic equations and leads to a reduction of the model size compared to the initial solid model.

First-order, as well as higher-order theories, can be considered. In this paper, we only use modified first-order theories.

A MATLAB© code produces the set of linear equations. In the Abaqus input file, these equations are introduced using the keyword 'EQUATION' [9].

4.2 DISTRIBUTIONS AND NODE LOCATIONS FOR SOLID-SHELL APPROACH

For the layers, the displacement field in Equation (1) was exploited by Wei et al. [7], using the Reissner-Mindlin theory [12,13], modified to correctly consider the Poisson effect through the thickness. The displacement field is linear through the thickness for *u* and *v* and quadratic for *w*.

$$\begin{cases} u(z) = za_1 + a_2 \\ v(z) = zb_1 + b_2 \\ w(z) = z^2c_1 + zc_2 + c_3 \end{cases} \quad (1)$$

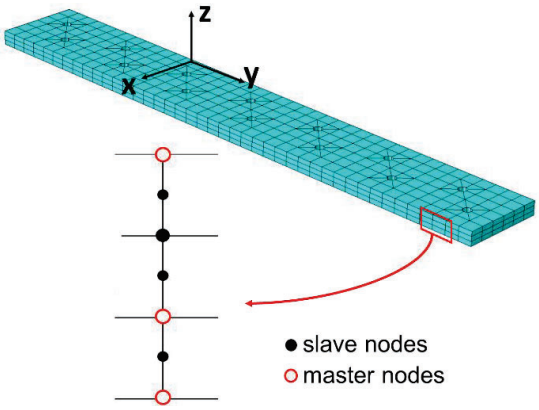

Figure 10: *Master and slave nodes locations for the modified first-order solid-shell approach*

The displacement field is applied through the thickness of a layer as represented in Figure 10. The coefficients in Equation (1) are identified using the coordinates of nodes and displacements at degrees of freedom of master nodes. Then this displacement field is applied to the degrees of freedom of slave nodes which are eliminated. The location of master and slave nodes is described in Figure 10.

4.3 DISTRIBUTIONS AND NODE LOCATIONS FOR SOLID-BEAM APPROACH

For the dowels, the displacement field in Equation (2) was exploited by Wei et al. [6], using the modified Timoshenko theory [14,15]. The reader can find complementary information in the paper by Wei et al. [6].

$$\begin{cases} u(y,z) = ya_1 + za_2 + a_3 \\ v(y,z) = y^2b_1 + z^2b_2 + yzb_3 + yb_4 + zb_5 + b_6 \\ w(y,z) = y^2c_1 + z^2c_2 + yzc_3 + yc_4 + zc_5 + c_6 \end{cases} \quad (2)$$

The displacement field in Equation (2) is applied through the cross-section of each dowel. The distribution is linear for *u* (longitudinal displacement) and quadratic for *v* and *w* (transverse displacement).

The same principle using slave and master nodes is applied again. Figure 11 describes the location of master and slave nodes.

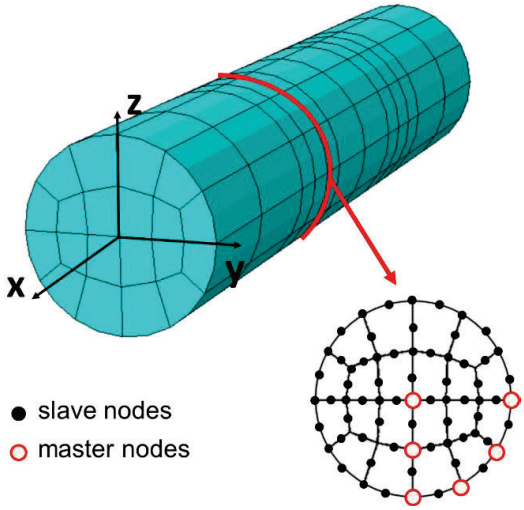

Figure 11: *Master and slave nodes locations for the modified first-order solid-beam approach*

4.4 RESULTS WITH REDUCED MODELS

The reference models respectively for AFLB and AFCLT panel are the ones described in section 3.2 and obtained with the Verification and Validation process. Reduced models for both AFLB and AFCLT panel are created using the methodology presented in sections 4.2 and 4.3. In this section, the reduced models are compared to the reference models. The quality of results and cost reduction are also highlighted.

4.4.1 AFLB reduced model

Table 6 compares, for AFLB, the numerical frequencies obtained with the reference and the reduced finite element

https://doi.org/10.52202/069179-0343

models. The difference between the two models in terms of quality is acceptable with a maximum difference of 5.8 % for the highest frequency.
The comparison of model size and computational cost is summarized in Table 7. The reduction in number of floating-point operations is 97 %. The number of degrees of freedom (d.o.f.) is reduced by 76 %.

Table 6: *Comparison of frequencies between the reference and the reduced models for the AFLB*

	Reference model	Reduced model	Diff.
f_1	119.1 Hz	121.1 Hz	1.7 %
f_2	278.2 Hz	290.0 Hz	4.2 %
f_3	459.6 Hz	486.4 Hz	5.8 %

Table 7: *Comparison of size and computational cost between the reference and the reduced models for the AFLB*

	Reference model	Reduced model	Reduction
Number of d.o.f.	221 220	53 553	76 %
Number of floating point operations	1.34×10^{11}	4.13×10^{9}	97 %

4.4.2 AFCLT panel reduced model

Table 8 compares, for AFCLT panel, the numerical frequencies obtained with the reference and the reduced finite element models. The frequencies obtained with the reduced and solid models are very close to each other. The maximum difference is 3.5 % for the highest frequency.
The comparison of model size and computational cost is summarized in Table 9. The number of d.o.f. and number of floating-point operations are reduced by 77 % and 96 % respectively.

Table 8: *Comparison of frequencies between the reference and the reduced models for AFCLT panel*

	Reference model	Reduced model	Diff.
f_2	54.3 Hz	55.6 Hz	2.4 %
f_3	55.9 Hz	56.2 Hz	0.5 %
f_7	108.6 Hz	112.4 Hz	3.5 %

Table 9: *Comparison of size and computational cost between the reference and the reduced models for the AFCLT panel*

	Reference model	Reduced model	Reduction
Number of d.o.f.	1 460 256	335 356	77.0 %
Number of floating point operations	1.49×10^{12}	6.03×10^{10}	96.0 %

The reduction level is comparable for beams and panels models. However, for cross-laminated timber panels, the size of the numerical models is much larger than for beams. Consequently, reducing the size of the model is even more interesting in this case, especially for a variability or optimization assessment.

4.5 DISCUSSION ON REDUCED MODELS BASED ON HIGHER-ORDER THEORIES

The difference between the reference models and the reduced models for both the AFLB and the AFCLT panel is acceptable in terms of quality. However, some might find it too high for a comparison between two finite element models. The reason for this slight discrepancy is due to the fact that only first-order theories are used here and applied to the totality of the layers and dowels.
Higher-order beam and shell, as well as a mix between beam, shell and solid theories, have also been considered. These other approaches allow us to obtain a better quality of results between the reference and reduced models but in that case, the reduction level is lower. In this paper, only modified first-order theories, which lead to the largest reduction level, are presented.

5 CONSIDERING VARIABILITY WITH A PROBABILISTIC APPROACH

Bui et al. [4] assessed the variability of the vibration frequencies of AFLB and AFCLT panel using the Modal Stability Procedure (MSP). Here, and based on this previous study, we recall the principle of the MSP. Then we apply it to calculate the variability of two frequencies of the AFCLT panel and compare it to the direct Monte Carlo Simulation (MCS).
One way to assess the variability is to use a probabilistic approach which assumes that statistical laws (distribution type, mean value, standard deviation) define the input parameters. Then, statistical characteristics of the output quantities are obtained.
The direct MCS is a robust probabilistic method. In this method, a large number of trials is required with random input values to estimate the statistical characteristics of the output quantities. The computational time of one analysis is multiplied by the number of trials. Consequently, this approach is very computationally time-consuming.
The MSP, a less time-consuming variability assessment methodology, is investigated here.

5.1 THE MODAL STABILITY PROCEDURE

The MSP methodology was developed by Arnoult et al. [16]. Its efficiency in terms of quality of results and computational cost has been proven in multiple studies.
MSP assumes that the mode shape does not change between the original structure (subscript 0) and a perturbated one (subscript p), so $\phi_p = \phi_0$. Consequently, this methodology requires only one finite element analysis in the nominal configuration to extract the mode shapes ϕ_0 and modal strains ε_0.
Thanks to the previous assumption, we obtain the perturbed natural angular frequency for a given mode

using the perturbed stiffness matrix K_p and the perturbed mass matrix M_p:

$$\omega_p^2 = \frac{\phi_0^T K_p \phi_0}{\phi_0^T M_p \phi_0} \quad (3)$$

Equation (3) can be transformed as a summation over all n elements of the finite element model. The elementary internal strain energy of an element j can be expressed as the integration over the elementary volume V_j of the product of the stresses by the strains. Using the generalized Hooke's law to developpe the stress, we then obtain our metamodel as follows:

$$\omega_p^2 = \frac{\sum_{j=1}^{n} \int_{V_j} \varepsilon_{0j}^T C_{pj} \varepsilon_{0j} dV}{\sum_{j=1}^{n} \phi_{0j}^T m_{pj} \phi_{0j}} \quad (4)$$

with C_{pj} the constitutive law matrix and m_{pj} the perturbed mass matrix of the j^{th} element.
The metamodel in Equation (4) is used in a fast MCS, allowing the evaluation of perturbed natural frequencies for each trial. The variability (mean value, standard deviation, coefficient of variation and distribution) of natural frequencies can subsequently be obtained.
Figure 12 presents a flowchart explaining the whole methodology.

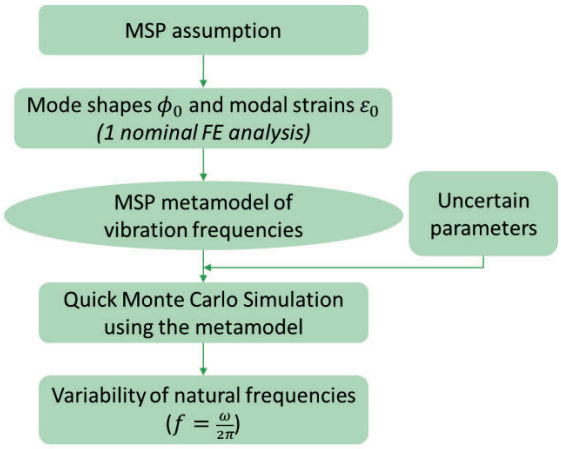

Figure 12: *MSP flowchart*

5.2 VARIABILITY OF AFCLT PANEL FREQUENCIES

The MSP results are presented for two frequencies of the AFCLT panel f_2 and f_3. The reference model is exploited here.

5.2.1 Inputs variability

Uncertain parameters are the material properties of dowels and boards. The parameters distribution is assumed to be Gaussian, however, the distribution law is truncated (±3σ) in order to avoid non-physical values.

Table 10 gives the mean value and coefficient of variation of the uncertain parameters. Four uncertain parameters are defined for each of the 28 boards and 3 uncertain parameters for each of the 196 dowels, leading to 700 independent uncertain parameters.

Table 10: *Variability levels of uncertain parameters*

		Mean value	CoV
board	ρ (kg/m^3)	624	6.5 %
	E_1 (MPa)	11400	13.6 %
	G_{12} (MPa)	1200	14 %
	G_{13} (MPa)	920	14 %
dowel	ρ (kg/m^3)	1133	4.2 %
	E_3 (MPa)	1100	9.5 %
	G_{13} (MPa)	800	10 %

5.2.2 Results

Simulations with 2000 trials using the MSP metamodel and the direct MCS are performed. Figure 13 illustrates the distribution of two frequencies.

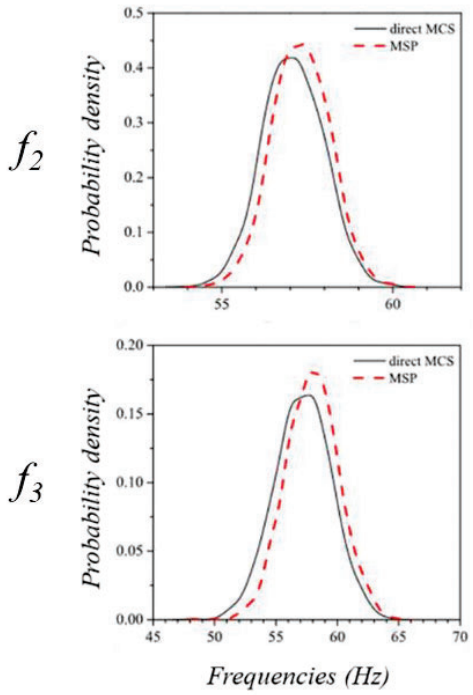

Figure 13: *Distribution of frequencies of AFCLT panel obtained with 2000 trials*

There is a good correlation between results obtained with MSP and direct MCS, even if limited shifts are observed. The maximal difference, observed for mode 3, is about 1 % for the mean value and 8 % for the standard deviation. MSP computational time is divided by about 1000 compared with direct MCS. We can thus conclude that MSP is satisfactory for the assessment of variability of frequencies of a AFCLT panel.

https://doi.org/10.52202/069179-0343

6 CONCLUSION AND PERSPECTIVES

Finite element models to assess the vibration behaviour of AFLB and AFCLT panel have been presented. The Verification and Validation approach shows that the reference model, composed of solid elements, is able to correctly reproduce the experimental frequencies.

A reduction technique, based on the application of solid-beam and solid-shell approaches for dowels and boards respectively, has been introduced. First-order beam and shell theories have been exploited, but higher-order theories can also be considered. The reduced finite element models show good results in terms of quality and significant model size and computational cost reduction compared to the reference models.

The MSP has been presented and applied to evaluate the variability of frequencies of a AFCLT panel using the reference models. The MSP is satisfactory in terms of quality and is much less time-consuming than the classical direct MCS approach.

A next step of this study will be to couple the MSP with reduced models.

Investigating the confrontation between experimental and numerical variability more deeply is also a perspective.

ACKNOWLEDGEMENT

The authors would like to thank the Hauts-de-France Region (France) and the Natural Sciences and Engineering Research Council of Canada (NSERC) for funding this work.

REFERENCES

[1] List of Classifications – IARC Monographs on the Identification of Carcinogenic Hazards to Humans. https://monographs.iarc.who.int/list-of-classifications.

[2] Bui T.A., Lardeur P., Oudjene M., Khelifa M., and Rogaume Y.: Towards experimental and numerical assessment of the vibrational serviceability comfort of adhesive free laminated timber beams and CLT panels assembled using compressed wood dowels. Eng. Struct., 216:110586, 2020.

[3] Bui T.A., Lardeur P., Oudjene M., Khelifa M., and Rogaume Y.: Vibration performance of adhesive free multi-layered timber beams assembled through compressed wood dowels. In: World Conference on Timber Engineering, 2018.

[4] Bui T.A., Lardeur P., Oudjene M., and Park J.: Numerical modelling of the variability of the vibration frequencies of multi-layered timber structures using the modal stability procedure. Compos. Struct., 285:115226, 2022.

[5] Bui T.A.: Experimental and numerical uncertain vibration analysis of multilayered timber structures assembled using compressed wood dowels. *PhD thesis*, University of Lorraine, 2020.

[6] Wei G., Lardeur P., and Druesne F.: A new solid-beam approach based on first or higher-order beam theories for finite element analysis of thin to thick structures. Finite Elem. Anal. Des., 200:103655, 2022.

[7] Wei G., Lardeur P., and Druesne F.: Solid-shell approach based on a first-order or higher-order plate and shell theories for the finite element analysis of thin to very thick structures. Eur. J. Mech. - ASolids, 94:104591, 2022.

[8] Lardeur P., Scigliano R., and Scionti M.: Verification and validation for the vibration study of automotive structures modelled by finite elements. J. Strain Anal. Eng. Des., 48:59-72, 2013.

[9] Simulia: ABAQUS Analysis User's Manual (version 6.14).

[10] Jodin P.: Le bois, matériau d'ingénierie. Association pour la recherche sur le bois en Lorraine Nancy, 1994.

[11] Bouhala L., Fiorelli D., Makradi A., Belouettar S., Sotayo A., Bradeley D.F., Guan Z..: Advanced numerical investigation on adhesive free timber structures. Compos. Struct., 246:112389, 2020.

[12] Reissner E.: The Effect of Transverse Shear Deformation on the Bending of Elastic Plates. J. Appl. Mech., 12(2):A69-A77, 1945.

[13] Mindlin R. D.: Influence of Rotatory Inertia and Shear on Flexural Motions of Isotropic, Elastic Plates. J. Appl. Mech., 18(1):31-38, 1951.

[14] Timoshenko S. P.: On the correction for shear of the differential equation for transverse vibrations of prismatic bars. Lond. Edinb. Dublin Philos. Mag. J. Sci., 41(245):744-746, 1921.

[15] Timoshenko S. P.: On the transverse vibrations of bars of uniform cross-section. Lond. Edinb. Dublin Philos. Mag. J. Sci., 43(253):125-131, 1922.

[16] Arnoult E., Lardeur P., and Martini L.: The modal stability procedure for dynamic and linear finite element analysis with variability. Finite Elem. Anal. Des., 47(1):30–45, 2011.